Full counting statistics of a nonadiabatic electron pump

Alexander Croy* and Ulf Saalmann
Max-Planck-Institute for the Physics of Complex Systems, Nöthnitzer Straße 38, D-01187 Dresden, Germany
(Received 20 August 2015; revised manuscript received 1 April 2016; published 20 April 2016)

Nonadiabatic charge pumping through a single-level quantum dot with periodically modulated parameters is studied theoretically. By means of a quantum-master-equation approach the full counting statistics of the system is obtained. We find a trinomial-probability distribution of the charge transfer, which adequately describes the reversal of the pumping current by sweeping the driving frequency. Further, we derive equations of motion for current and noise and solve those numerically for two different driving schemes. Both show interesting features, which can be fully analyzed due to the simple and generic model studied.

DOI: 10.1103/PhysRevB.93.165428

I. INTRODUCTION

Pumping of electrons through nanodevices by a time-dependent modulation of device parameters has received a lot of interest over the past years. Such pumps are interesting for many applications, but they are particularly useful in metrology [1,2]. In this context, experimental and technological progress has lead to both high-frequency (in the GHz regime) [3–6] and high-accuracy charge pumping [7] and opened the path for on-demand single-electron sources [8,9]. For a review see Ref. [10].

Moreover, pumping is also interesting for addressing fundamental questions connected with the transport of quantum particles. Knowledge about the full counting statistics (FCS) of the pumped electrons allows a detailed understanding of relaxation and quantum effects [11]. FCS for Coulomb-blockade systems has been studied theoretically in the context of stationary [12–14], driven [15–17], and nanoelectromechanical [18–20] systems. In particular, understanding the noise of the pumping current is relevant for high-accuracy pumping. Accordingly, the noise in different setups of driven devices has been investigated theoretically [21–23] and measured, for example, in a charge pump [24].

While adiabatic pumping is very well studied [25–32], the description of nonadiabatic effects remains challenging. In view of the experimental developments toward higher frequencies, this regime becomes increasingly relevant [10]. Moreover, nonadiabatic driving can lead to interesting effects [29,33], like the possibility to reverse the pumping current by sweeping the driving frequency [34]. In order to exploit such effects a better understanding of the FCS for fast pumping is necessary.

In this article we consider an electron pump modeled by a single-level quantum dot at zero bias. In a previous study [34] we focused on the pumped charge per cycle in the nonadiabatic regime. We showed that the pumping current vanishes for a certain driving frequency, but to identify the underlying mechanism one has to go beyond current calculations. Based on the formalism given before [18] we calculate the cumulant-generating function at zero temperature and for arbitrary driving schemes. We show that in the adiabatic regime, the probability distribution for pumping electrons is always binomial, which implies that the pumping can be regarded as being unidirectional. In the nonadiabatic regime we obtain a trinomial distribution, which also explains the occurrence of the current reversal [34]. We show that fluctuations at the reversal may show either a minimum or a maximum, depending on the driving scheme.

The outline of the article is as follows. In the next section we derive the FCS for a quantum-dot electron pump. We also discuss the calculation of the pumping-current noise. In Sec. III we consider a specific time-dependence of the tunneling rates and the dot energy and compare the numerical results for this model to the analytic expressions obtained in Sec. II. Finally, we conclude with a summary and a discussion.

II. THEORY

We consider a resonant-level model [34] characterized by a time-dependent energy level $\varepsilon(t)$ and time-dependent couplings to the left and right reservoirs given by tunneling rates $\Gamma_{\mathrm{L}}(t)$ and $\Gamma_{\mathrm{R}}(t)$, respectively. As indicated, these parameters explicitly depend on time. The actual time dependence will be specified below. In the following we focus on the fully spin-polarized case, which is easier to analyze. The more general case is treated in the Appendix. The results are found to be qualitatively similar to the spinless situation and therefore it is sufficient do discuss the simpler case.

In order to obtain the FCS we consider the number of electrons N tunneling through the left barrier. Note that, in general, this number is different for the right barrier. However, time-averaged quantities in the steady-state regime do not depend on the barrier (left or right) they are calculated for. The statistics of N can be found from the characteristic function $\Phi(\chi,t) \equiv \langle \exp[\mathrm{i}\chi N]\rangle$, where χ is the counting variable. Knowing $\Phi(\chi,t)$, one can deduce the moments $\langle N^m(t)\rangle$ by differentiation.

We are interested in a regime, where the Coulomb blockade picture is valid and Kondo physics is not relevant. This implies that the coupling-rate to the leads (Γ) is smaller than the single-level spacing (δ) and smaller than the charging energy (U); the temperature (T) has to be larger than the Kondo temperature (T_{K}). In the present case, the driving amplitude ε_1 gives rise to another energy scale, which is larger than Γ and smaller than U and δ.

Under those conditions, which imply short reservoir correlation-time and Coulomb blockade, the characteristic

*croy@pks.mpg.de

 ©2016 American Physical Society

function for the present model can be determined from the following equation [12]:

$$\frac{\partial}{\partial t}\begin{pmatrix} p_0(\chi,t) \\ p_1(\chi,t)\end{pmatrix} = -\mathbb{L}_\chi(t)\begin{pmatrix} p_0(\chi,t) \\ p_1(\chi,t)\end{pmatrix}, \quad \text{with} \quad \mathbb{L}_\chi(t) \equiv \begin{Bmatrix} f(t)\Gamma(t) & -\bar{f}(t)\left[e^{-i\chi}\Gamma_L(t)+\Gamma_R(t)\right] \\ -f(t)[e^{i\chi}\Gamma_L(t)+\Gamma_R(t)] & \bar{f}(t)\Gamma(t)\end{Bmatrix}, \tag{1a}$$

where we have used

$$f(t) \equiv \frac{1}{1+\exp(\varepsilon(t)/k_BT)}, \quad \bar{f}(t) \equiv 1-f(t), \tag{1b}$$

$$\Gamma(t) \equiv \Gamma_L(t)+\Gamma_R(t). \tag{1c}$$

Note that the counting field χ "measures" tunneling from and to the left reservoir only. For $\chi = 0$, Eq. (1) reduces to the usual (Markovian) master equation for the diagonal elements of the reduced density matrix [35]. In this case, the components of the vector $\mathbf{p} = (p_0, p_1)^t$ correspond to $p_0(t) = 1 - n(t)$ and $p_1(t) = n(t)$ with $n(t)$ the average occupation of the level at time t. The characteristic function is given in terms of the solution $\mathbf{p}$ of Eq. (1)

$$\Phi(\chi,t) = \mathbf{q}\,\mathbf{p}(\chi,t) \quad \text{with} \quad \mathbf{q} = (1,1). \tag{2}$$

The product is to be understood as a scalar product of two two-component vectors.

Provided, that all external parameters change periodically with frequency Ω, we can substitute $\phi = \Omega t$ to get [18]

$$\frac{\partial}{\partial\phi}\mathbf{p}(\chi,\phi) = -\frac{1}{\Omega}\mathbb{L}_\chi(\phi)\mathbf{p}(\chi,\phi), \tag{3}$$

with $\mathbb{L}_\chi$ defined in Eq. (1). The solution after one cycle can be written as $\mathbf{p}(\chi,\phi+2\pi) = \mathbb{A}\,\mathbf{p}(\chi,\phi)$ with the matrix

$$\mathbb{A} \equiv \mathcal{T}\exp\left[-\frac{1}{\Omega}\int_0^{2\pi} d\phi\;\mathbb{L}_\chi(\phi)\right], \tag{4}$$

where $\mathcal{T}$ denotes the time-order prescription.

Assuming that the counting fields can be switched on and off adiabatically, the generating function for k counting cycles is obtained from [12,18]

$$\Phi_k = \mathbf{q}\,\mathbb{A}^k\,\tilde{\mathbf{p}}, \tag{5}$$

where $\tilde{\mathbf{p}}$ is the steady-state solution for $\chi = 0$. For a large number of cycles k the characteristic function is determined by the largest eigenvalue [12,18] of $\mathbb{A}$.

A. Current and noise

For many applications it is sufficient to know the first two moments, $Q = \langle N\rangle$ and $\Delta Q^2 = \langle \Delta N^2\rangle$, of the pumped charge. The moments are given in units of e and e^2. In the following, we will first derive a set of equations that allow the calculation of both moments for arbitrary frequencies and temperatures. Since we assumed the counting to occur in the left reservoir, all time-dependent quantities refer to that reservoir and the label is suppressed.

As will be shown, it is more convenient to consider the time-derivatives, $I(t) = \partial_t\langle N\rangle$ and $S(t) = \partial_t\langle \Delta N^2\rangle$. Starting from the definition of the current, one gets the following expression:

$$\begin{aligned} I(t) &= \frac{\partial}{\partial t}\langle N\rangle = \mathbf{q}\frac{\partial}{\partial t}\frac{\partial}{\partial(i\chi)}\mathbf{p}\Big|_{\chi=0} = -\mathbf{q}\frac{\partial\mathbb{L}_\chi}{\partial(i\chi)}\mathbf{p}\Big|_{\chi=0} \\ &= \Gamma_L(t)[f(t)-n(t)], \end{aligned} \tag{6}$$

where we have used Eq. (1) and $\mathbf{q}\,\mathbb{L}_{\chi=0} = (0,0)$. Similarly, one finds

$$\begin{aligned} S(t) &= \frac{\partial}{\partial t}[\langle N^2\rangle - \langle N\rangle^2] = \mathbf{q}\left[\frac{\partial}{\partial t}\frac{\partial^2}{\partial(i\chi)^2} - 2I\frac{\partial}{\partial(i\chi)}\right]\mathbf{p}\Big|_{\chi=0} \\ &= -\mathbf{q}\left[\frac{\partial^2\mathbb{L}_\chi}{\partial(i\chi)^2} + 2\frac{\partial\mathbb{L}_\chi}{\partial(i\chi)}\frac{\partial}{\partial(i\chi)} + 2I\frac{\partial}{\partial(i\chi)}\right]\mathbf{p}\Big|_{\chi=0} \\ &= -2\Gamma_L(t)r(t) + \Gamma_L(t)[\bar{f}(t)n(t) + f(t)\bar{n}(t)], \end{aligned} \tag{7}$$

where

$$r(t) \equiv p_1'(t) - n(t)[p_0'(t)+p_1'(t)], \tag{8a}$$

$$p_j'(t) \equiv \frac{\partial p_j(\chi,t)}{\partial(i\chi)}\Big|_{\chi=0} \quad \text{for } j = 0,1. \tag{8b}$$

To calculate I and S, the time evolution of the occupation n and the newly defined quantity r are needed. Both of them can be obtained from Eq. (1). For $n(t)$ one can use the lower component of Eq. (1a) for $\chi\to 0$. For $r(t)$ one needs the time derivative of $\mathbf{p}' = (p_0', p_1')^t$, which is obtained from the derivative of Eq. (1a) with respect to χ in the limit $\chi\to 0$, i. e., $\frac{\partial}{\partial t}\mathbf{p}'(t) = -\mathbb{L}_0'(t)\mathbf{p}(0,t) - \mathbb{L}_0(t)\mathbf{p}'(t)$. The corresponding equations are

$$\frac{\partial}{\partial t}n(t) = \Gamma(t)[f(t)-n(t)], \tag{9a}$$

$$\frac{\partial}{\partial t}r(t) = -\Gamma(t)r(t) + \Gamma_L(t)[f(t)\bar{f}(t) + [f(t)-n(t)]^2]. \tag{9b}$$

Equations (9) can be solved numerically in a straightforward way. The moments Q and ΔQ^2 are found by integrating I and S over one period, respectively. For low frequencies and finite temperatures, one can obtain analytical expressions for both quantities. This case is discussed in Sec. II C below.

B. FCS at zero temperature

In the following section we calculate the generating function at zero temperature, i.e., when the Fermi function only attains the values 0 and 1. To this end we assume that for $0 \leqslant \phi < \pi$ the level is charged ($f = 1$, $\bar{f} = 0$) and for $\pi \leqslant \phi < 2\pi$ it is decharged ($f = 0$, $\bar{f} = 1$). In this case, the solutions to Eq. (1) at the end of the respective half-periods can be obtained analytically. Overall, we get for one period

$$\mathbf{p}(\chi,2\pi) = \mathbb{A}_0(\chi)\mathbf{p}(\chi,0), \quad \text{with} \quad \mathbb{A}_0(\chi) \equiv \begin{pmatrix} 1-\beta_L-\beta_R+(e^{-i\chi}\gamma_L+\gamma_R)(e^{i\chi}\beta_L+\beta_R) & e^{-i\chi}\gamma_L+\gamma_R \\ (1-\gamma_L-\gamma_R)(e^{i\chi}\beta_L+\beta_R) & 1-\gamma_L-\gamma_R\end{pmatrix}, \tag{10a}$$

and the abbreviations

$$\beta_\alpha \equiv \int_0^\pi d\phi\, \frac{\Gamma_\alpha(\phi)}{\Omega} \exp\left[-\frac{1}{\Omega}\int_0^\phi d\phi'\, \Gamma(\phi')\right],$$
$$\gamma_\alpha \equiv \int_\pi^{2\pi} d\phi\, \frac{\Gamma_\alpha(\phi)}{\Omega} \exp\left[-\frac{1}{\Omega}\int_\pi^\phi d\phi'\, \Gamma(\phi')\right]. \quad (10b)$$

Note that β_α and γ_α are completely determined by the time-dependence of the rates Γ_α. They define probabilities for charging or decharging the level either from the left or the right reservoir, respectively. Obviously, $\beta_\alpha, \gamma_\alpha > 0$. Further, we note that

$$\beta_L + \beta_R = 1 - \exp\left(-\frac{1}{\Omega}\int_0^\pi d\phi'\, \Gamma(\phi')\right) < 1. \quad (11)$$

Since both quantities, β_L and β_R, are positive it follows from Eq. (11) that $\beta_L, \beta_R < 1$. Similar arguments hold for γ_L and γ_R. In order to simplify the notation, in the following we use the definitions

$$\bar\beta \equiv 1 - \beta_L - \beta_R, \quad \bar\gamma \equiv 1 - \gamma_L - \gamma_R. \quad (12)$$

Finally, the eigenvalues of the zero-temperature matrix $\mathbb{A}_0(\chi)$, which is defined in Eq. (10a), are given by

$$\lambda_\pm = \tfrac{1}{2}[g(\chi) \pm \sqrt{g^2(\chi) - 4\bar\beta\bar\gamma}], \quad (13a)$$
$$g(\chi) \equiv \bar\beta + \bar\gamma + (e^{-i\chi}\gamma_L + \gamma_R)(e^{i\chi}\beta_L + \beta_R), \quad (13b)$$

from which the current and noise can be obtained by differentiation. The eigenvalue with the largest absolute value is λ_+. This expression is exact under the assumptions stated above and can be used to obtain the FCS of the pumped charge.

To gain further insight about the nature of the statistics, it is useful to consider limiting cases. If $\bar\beta, \bar\gamma \ll 1$ one can write down the following generating function:

$$(\Phi_k)^{1/k} \approx \gamma_L\beta_R e^{-i\chi} + \beta_L\gamma_R e^{i\chi} + (\bar\beta + \bar\gamma + \beta_L\gamma_L + \beta_R\gamma_R). \quad (14)$$

This limit describes the situation where the level is almost fully charged in the first half cycle and correspondingly decharged in the second half cycle. Note that the expression in Eq. (14) yields $\Phi_k \approx 1$ for $\chi = 0$ only to first order in $\bar\beta, \bar\gamma$.

Equation (14) characterizes a trinomial probability distribution. Accordingly, there are three relevant probabilities,

$$p_- = \gamma_L\beta_R,\ p_+ = \beta_L\gamma_R, \text{ and } p_0 = 1 - p_- - p_+, \quad (15)$$

which describe a process of an electron being transferred to the left reservoir, to the right reservoir, or no transfer, respectively. It follows that the average charge and noise per period are

$$Q = p_+ - p_-, \quad (16a)$$
$$\Delta Q^2 = p_+(1-p_+) + p_-(1-p_-) + 2p_+p_-. \quad (16b)$$

For $p_+ = p_-$ one finds that the pumped charge vanishes, $Q = 0$, while the noise remains finite, $\Delta Q^2 = 2p_+$ for $p_+ > 0$. At the vicinity of this point one obtains a current reversal [33,34].

In the opposite limit, $\bar\beta, \bar\gamma \approx 1$, where the energy level is nearly empty during one cycle, one can approximate the generating function by

$$(\Phi_k)^{1/k} = c + \sqrt{(e^{-i\chi}\gamma_L + \gamma_R)(e^{i\chi}\beta_L + \beta_R)}. \quad (17)$$

Here, c is independent of χ and guarantees $\Phi_k|_{\chi=0} = 1$. Equation (17) describes in general a complicated probability distribution. However, if one barrier is dominating the charging and the other one dominates the decharging, one obtains a binomial distribution for a half-charge transfer. For example, if $\beta_R \approx \gamma_L \approx 0$ one gets

$$(\Phi_k)^{1/k} \approx c' + e^{i\chi/2}\beta_L\gamma_R. \quad (18)$$

This "fractional" behavior has been discussed previously in the context of charge pumping [36] and nanoelectromechanical charge shuttles [18]. It reflects the fact that the cycles are no longer independent of each other. For many counting cycles, however, the behavior can effectively be described by the independent transfer of fractional charges. For later reference we note that the charge per cycle can be obtained from Eq. (17) to read

$$Q = \frac{\beta_L\gamma_R - \beta_R\gamma_L}{2\sqrt{(\beta_L+\beta_R)(\gamma_L+\gamma_R)}}. \quad (19)$$

C. Noise for low frequencies and finite temperatures

At low frequencies, it is sufficient to consider the instantaneous contribution from Eqs. (9), as done similarly before [30]. Consequently, the time-derivatives are set to zero and one obtains

$$n(t) = f(t), \quad \Gamma(t)r(t) = \Gamma_L(t)f(t)\bar f(t). \quad (20)$$

The instantaneous current and noise become

$$I(t) = 0, \quad S(t) = \frac{2f(t)\bar f(t)}{1/\Gamma_L(t) + 1/\Gamma_R(t)}. \quad (21)$$

Not surprisingly, the current is zero, since the level is at all times in equilibrium with the reservoirs. The noise is nonzero and is called equilibrium, or Nyquist-Johnson noise [37]. It is caused by the statistical nature of the electron occupation in the reservoirs characterized by the Fermi distribution. Using the property $f\bar f = -k_BT\frac{\partial f}{\partial\varepsilon}$ the expression for the noise becomes

$$S(t) = -2k_BT\frac{1}{1/\Gamma_L(t) + 1/\Gamma_R(t)}\frac{\partial f}{\partial\varepsilon}. \quad (22)$$

The noise per period is obtained from integrating over one period,

$$\Delta Q^2 = -2\frac{k_BT}{\Omega}\int_0^{2\pi} d\phi\, \frac{[\partial\varepsilon(\phi)/\partial\phi]^{-1}[\partial f(\phi)/\partial\phi]}{1/\Gamma_L(\phi) + 1/\Gamma_R(\phi)}. \quad (23)$$

The integral gives a value that is independent of Ω but depends on the details of the external driving, i.e., the time-dependent level and tunneling rates. Consequently, the noise per period will be proportional to k_BT/Ω.

III. RESULTS

We study the first two cycle-averaged moments of the FCS: the charge Q and its fluctuations ΔQ^2 for an electron pump that shows current reversal and rectification effect in the nonadiabatic regime [34]. They are obtained by integrating $I(t)$ and $S(t)$, as given by Eqs. (6) and (7), respectively, over

one cycle under steady-state conditions, i.e., $\tilde{\mathbf{p}}(\phi) = \mathbb{A}\,\tilde{\mathbf{p}}(\phi)$ with $\mathbb{A}$ defined in Eq. (4).

A. Exponential modulation

To this end, Eq. (9) has been integrated numerically with the following pumping parameters:

$$\varepsilon(t) = 20\Gamma\cos(\Omega t), \tag{24a}$$

$$\Gamma_{\mathrm{L}}(t) = [\Gamma/2]\exp(6[\cos(\Omega t - \delta) - 1]), \tag{24b}$$

$$\Gamma_{\mathrm{R}}(t) = [\Gamma/2]\exp(6[\cos(\Omega t) - 1]). \tag{24c}$$

The same parameters have been used before [34]. They allow for the exponential dependence of tunneling rates due to oscillatory gate voltages as used in the experiments of Refs. [5,6]. The pumping is characterized by two parameters, the driving frequency Ω and the time or phase delay δ of the left barrier with respect to the right one. The latter one is locked to the level ε, which oscillates around the Fermi energy of both reservoirs $\mu_{\mathrm{L}} = \mu_{\mathrm{R}} = 0$. If not specified differently, the temperature in the contacts is $k_{\mathrm{B}}T = \Gamma/100$.

Figure 1 gives an overview of the results. We have varied the frequency Ω in a rather large range (10^{-5}... 10 Γ) in order to cover the asymptotic adiabatic and nonadiabatic behavior for low and high frequencies, respectively. One can clearly see [Fig. 1(a)] that the direction of the charge transport does not only depend on the phase delay δ, which controls the oscillation of the left barrier with respect to the right one.

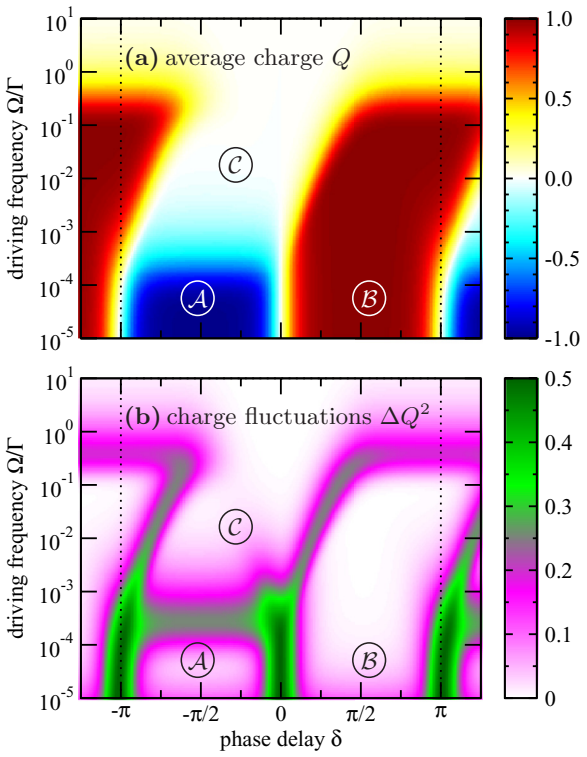

FIG. 1. Pumped charge Q and fluctuations ΔQ^2 as a function of phase delay δ and driving frequency Ω as obtained with the set of Eqs. (6)–(9) for the time dependence of quantum-dot level ε and couplings $\Gamma_{\mathrm{R,L}}$ given in Eqs. (24).

Rather the frequency Ω is equally important and may be used to cause a current reversal as was discussed in detail before [34].

The charge fluctuations [Fig. 1(b)] show a similar pattern as the average charge, albeit somehow inverted. Not surprisingly they vanish [white areas in Fig. 1(b)], when the charge transport is *quantized* either to the left [blue areas marked with $\mathcal{A}$ in Fig. 1(a)] or to the right [red areas marked with $\mathcal{B}$ in Fig. 1(a)] direction. In regions, however, where this is not the case the fluctuations are finite, reaching sometimes a value of $\Delta Q^2 = 1/2$.

One maybe tempted to explain the charge fluctuations with the well-known expression for a binomial distribution [38],

$$\Delta Q^2 = p\,(1 - p), \tag{25}$$

with p the probability to transfer one charge per cycle. It is $p = |Q| = |p_+ - p_-|$ with $p_\pm$ defined in Eq. (15). The binomial distribution is expected to work if there are only two possibilities for the transport, e.g., transport in one direction or no transport. As we will see this binomial description is only applicable for finite values of Q. It fails in regions where the current changes direction, i. e., where $Q = 0$. To account for the reversal, a trinomial description is required. The charge can be transferred from left to right or right to left or no transfer can occur. The charge per cycle vanishes when the pumping currents in either direction compensate each other. However, the fluctuations ΔQ^2 remain nonzero, since there is still transfer of charges. There are two exceptions where Q and ΔQ^2 vanishes simultaneously. One is the region marked with $\mathcal{C}$ in Fig. 1 and the other one is the high-frequency regime where $\Omega \gg \Gamma$. We will discuss all regions in the following. To be more quantitative we have plotted the charge fluctuations for selected phase delays of $\delta = -3\pi/4$, $\delta = 0$, and $\delta = +\pi/2$, respectively, in Fig. 2.

For $\delta = -3\pi/4$ there is a current reversal at $\Omega \approx 5\times10^{-3}\Gamma$ [cf. upper panel in Fig. 2(a)]. Along with the result from the rate equations (Fig. 1 and thick gray line in Fig. 2) we show the binomial expression Eq. (25) and the trinomial expression from Eq. (16b). The values of p_+ and p_- in the latter case have been calculated numerically. Note that this is an approximation since we have assumed $k_{\mathrm{B}}T = 0$ in defining $p_\pm$. Both shot-noise models agree qualitatively with the numerical result. However, at the current reversal ($Q = 0$) charge fluctuations ΔQ^2 are on the order of 1/10, i. e., they do not vanish as predicted by Eq. (25). The trinomial description Eq. (16b) captures this behavior even quantitatively as Fig. 2(a) shows. Thus, the fluctuations reveal that the vanishing net transfer is not due to the fact that there is no transfer at all. Rather transfer to the right and to the left do cancel each other exactly.

The discrepancy between binomial and trinomial description becomes even more obvious for $\delta = 0$, which is shown in Fig. 2(b). Due to symmetry ($p_+ = p_-$) the charge Q vanishes for all frequencies Ω and so does the binomial expression Eq. (25). In contrast, the trinomial expression, which simplifies to $\Delta Q^2 = 2p_+ = 2p_-$, describes the fluctuations for all frequencies even quantitatively. Compared to the frequency-driven current reversal in Fig. 2(a) the fluctuations are even larger here.

The case $\delta = +\pi/2$, shown in Fig. 2(c), is characterized by a quantized and thus fluctuation-free transfer over a wide range of frequencies ($\Omega \approx 10^{-5} \ldots 10^{-1}\Gamma$).

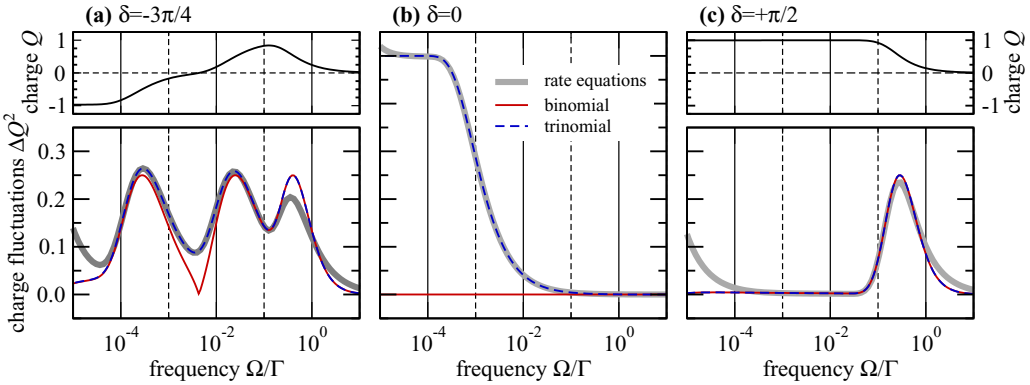

FIG. 2. Charge fluctuations Eq. (7) obtained from the rate equations [Eqs. (9)] for three selected phase delays δ and $k_B T = \Gamma/100$. They are compared to those obtained for a trinomial probability distribution Eq. (16) with $p_- = \gamma_L \beta_R$, $p_+ = \beta_L \gamma_R$ and a binomial distribution function Eq. (25) with $p \equiv |p_+ - p_-|$.

It remains to discuss the case where Q and ΔQ^2 vanish simultaneously. For large frequencies this is rather obvious, p_+ and p_- become small for $\Omega \gg \Gamma$ since the transfer to either side can be neglected. It is less clear for the region marked with $\mathcal{C}$. It can be traced back to the coupling to right contact: both β_R and γ_R, as defined in Eq. (10b), do vanish. If the level can neither be charged from the right (β_R) nor decharged to the right (γ_R), the probabilities of transfer from (p_+) and to (p_-) the right contact do vanish as well.

Careful inspection shows that for all three cases the fluctuations increase above the values predicted by the two shot-noise models. The reason is that thermal or Nyquist-Johnson noise $\Delta Q^2_{\text{therm}}$ starts to become larger than the shot noise. This is shown in Fig. 3, where thermal contribution according to Eq. (23) is shown separately with dashed lines. Clearly this occurs for larger temperatures $k_B T$ at higher frequencies Ω. The frequency, at which this takeover occurs, depends on the phase delay δ, as the three panels of Fig. 3 show. Above this critical frequency the noise spectrum is temperature-independent and well described by the zero temperature case considered in Sec. II B.

B. Harmonic modulation

Taking, instead of Eqs. (24b) and (24c),

$$\Gamma_\alpha(t) = \Gamma_0 + \Gamma_1 \cos(\Omega t + \pi/2 - \delta_\alpha), \tag{26}$$

yields a harmonic variation of the coupling rates, which is frequently used for modeling electron pumps. The same setup has been investigated in view of a current reversal before [34]. Using the same approach as in the last section, we calculate Q and ΔQ^2 for $\Gamma_0 = \Gamma_1 = \Gamma/20$, $\delta_R = 0$, and $\delta_L = \delta$. The results for a temperature of $k_B T = \Gamma/1000$ are shown in Fig. 4.

In all three cases, the fluctuations obtained from the trinomial probability distribution Eq. (16) agree very well with the results of the rate equations [Eqs. (9)]. Comparing to Fig. 2 one sees that the results are qualitatively similar for $\delta = 0$ and $\delta = \pi/2$. In the latter case and for harmonic modulation the fluctuations do not become zero in the adiabatic regime since the pumped charge is not quantized [cf. upper panel in Fig. 4(c)] in contrast to the exponential driving [cf. upper panel in Fig. 2(c)].

The biggest qualitative difference is observed for $\delta = -3\pi/4$. For harmonic modulation the charge fluctuations display a single maximum, which is attained in the vicinity of the current reversal. This is in contrast to the exponential modulation, where the fluctuations were found to have a minimum. This difference is connected with the behavior of the left and right probabilities $p_\pm$ in the vicinity of the reversal frequency Ω_*. It turns out that the slopes have the same magnitude but different signs. The curvatures may be different. Therefore, we consider the following simple Ω-dependence:

$$p_\pm(\Omega) = p_* \pm p'_*[\Omega - \Omega_*] + p''_{*\pm}[\Omega - \Omega_*]^2, \tag{27}$$

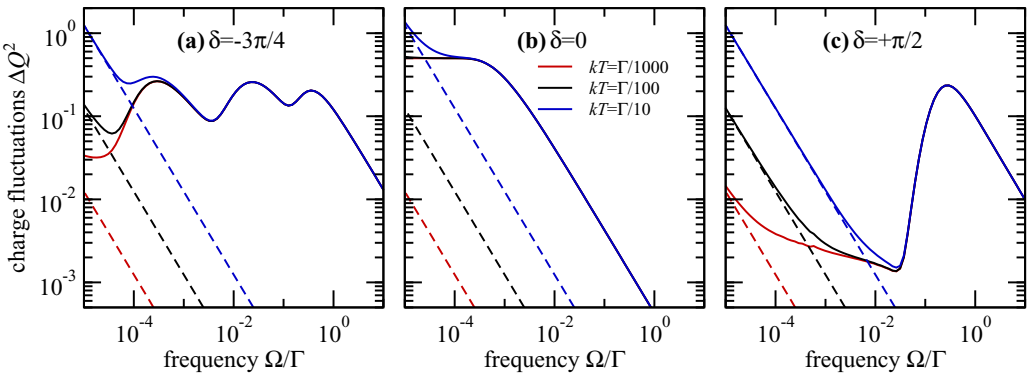

FIG. 3. Charge fluctuations as shown in Fig. 2, here with a double-logarithmic plot and for two additional temperatures $k_B T = \Gamma/1000$ and $k_B T = \Gamma/10$, respectively. The dashed lines show thermal noise according to Eq. (23).

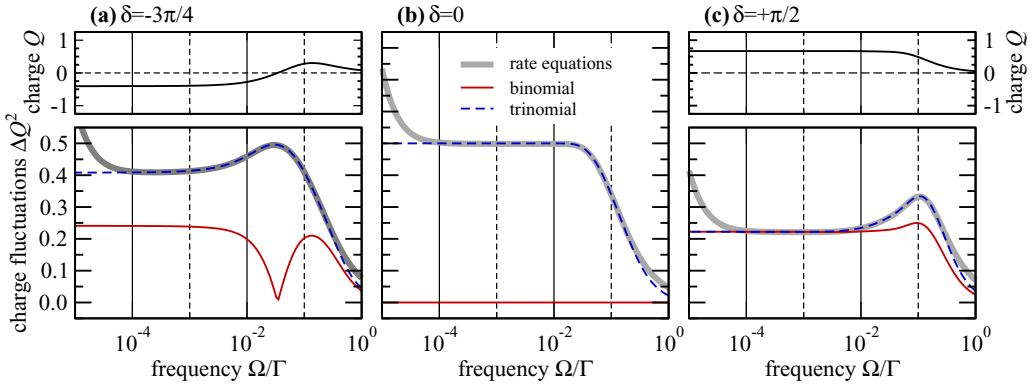

FIG. 4. Charge fluctuations Eq. (7) for harmonic modulation Eq. (26) of the tunneling rates obtained from the rate equations [Eqs. (9)] for three selected phase delays δ and $k_B T = \Gamma/1000$. They are compared to those obtained for a trinomial probability distribution Eq. (16) with $p_- = \gamma_L \beta_R$, $p_+ = \beta_L \gamma_R$, and a binomial distribution function Eq. (25) with $p \equiv |p_+ - p_-|$.

with $p_* = p_\pm(\Omega_*)$ and $Q(\Omega_*) = 0$. For such a parametrization the noise Eq. (16b) becomes up to second order,

$$\Delta Q^2(\Omega) \approx 2p_* - [4p_*'^2 - p_*''][\Omega - \Omega_*]^2, \tag{28}$$

where the abbreviation $p_*'' \equiv p_{*+}'' + p_{*-}''$ was used. The noise has an extremum at Ω_*, which can be a minimum or maximum depending on the relation of $4p_*'^2$ and p_*''. Whereas in the harmonic case the curvatures of $p_\pm$ at Ω_* have different signs but similar magnitudes, and thus $p_*'' \approx 0$, the situation in the exponential case is different. Here one finds a nonlinear increase or decrease of $p_\pm$ with $p_*'' \gg 4p_*'^2$. Correspondingly, close to the reversal we observe a maximum and a minimum of $\Delta Q^2(\Omega)$, respectively.

IV. SUMMARY AND CONCLUSIONS

In summary, we have investigated the counting statistics for nonadiabatic pumping of electrons through a single-level quantum dot. For zero temperature we derived an analytic expression for the generating function [Eq. (13)] in terms of the probabilities for charging or decharging the level during one pump cycle. In the case where those probabilities are large (the level is almost completely filled and emptied), we found a trinomial probability distribution for the charge transfer. The associated elementary processes correspond to an electron being transferred to the left reservoir, to the right reservoir, or no transfer. This has the important consequence that the transferred charge per cycle can vanish while the charge fluctuations remain finite. It also shows that the current-reversal does not rely on interference effects.

Our findings are corroborated by numerical simulations of the first two moments, Q and ΔQ^2, for two driving schemes (exponential and harmonic). To this end we derived a set of ordinary differential equations, valid for arbitrary time dependencies, which were solved numerically. Those equations may also be used in connection with pulse-shaping techniques, which allow for optimizing the pumping accuracy [7].

Our calculations show that the driving frequency and the phase delay are important parameters, both of which influence the *statistics* of the pumping charge. This demonstrates that the ability to control the phase delays potentially provides an additional knob to improve the performance of electron pumps.

APPENDIX: COULOMB-BLOCKADE

For a Coulomb-blockade system, where the energy level can be occupied by an electron with spin-up or spin-down, the matrix $\mathbb{L}_\chi$ becomes

$$\mathbb{L}_\chi(t) \equiv \begin{pmatrix} f(t)\Gamma(t) & -\xi_\uparrow \bar{f}(t)[e^{-i\chi}\Gamma_L(t)+\Gamma_R(t)] & -\xi_\downarrow \bar{f}(t)[e^{-i\chi}\Gamma_L(t)+\Gamma_R(t)] \\ -\xi_\uparrow f(t)[e^{i\chi}\Gamma_L(t)+\Gamma_R(t)] & \xi_\uparrow \bar{f}(t)\Gamma(t) & 0 \\ -\xi_\downarrow f(t)[e^{i\chi}\Gamma_L(t)+\Gamma_R(t)] & 0 & \xi_\downarrow \bar{f}(t)\Gamma(t) \end{pmatrix}. \tag{A1}$$

Here the coupling of the respective spin to the contacts is given by

$$\xi_{\uparrow\downarrow} = \frac{1 \pm \xi}{2}, \tag{A2}$$

and can be controlled by means of the parameter $\xi = -1 \ldots + 1$. The cases $\xi = -1$ or $\xi = +1$ refer to the fully polarized situation discussed in the main text, the case $\xi = 0$ means unpolarized pumping. Now, $\mathbf{p}$ has three components $\mathbf{p} = (n_0, n_\uparrow, n_\downarrow)^t$ and $\mathbf{q} = (1,1,1)$. It is convenient to introduce the following notation:

$$n_s(t) \equiv n_\uparrow(t) + n_\downarrow(t), \quad \delta n(t) \equiv n_\uparrow(t) - n_\downarrow(t). \tag{A3}$$

Analogously to the procedure presented in Sec. II A, one finds from Eqs. (6) and (7) for the current and the noise

$$I(t) = \frac{\Gamma_L(t)}{2}[f(t)[2 - n_s(t) + \xi\, \delta n(t)] - [n_s(t) + \xi\, \delta n(t)]], \tag{A4}$$

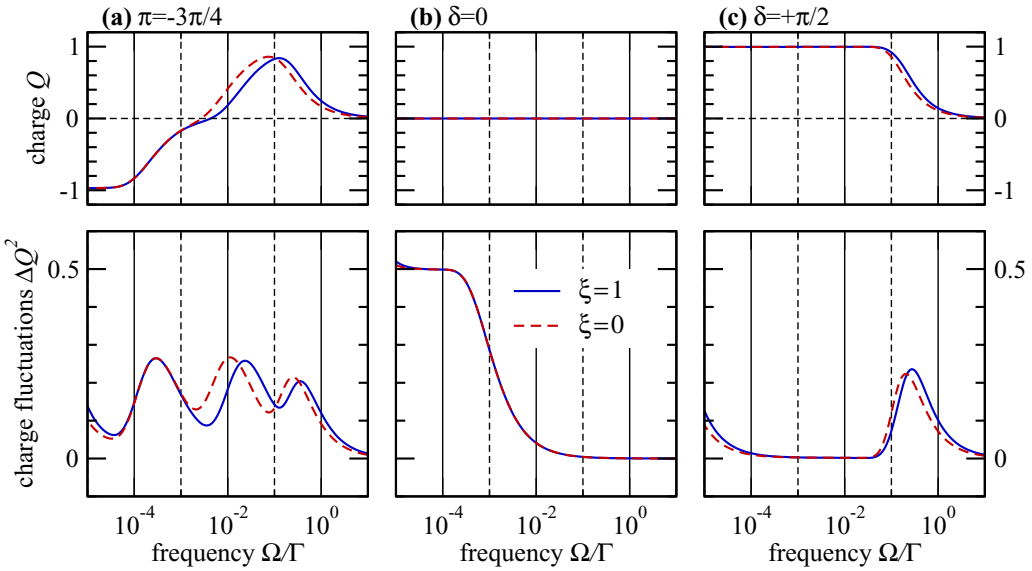

FIG. 5. Same quantities as in Fig. 2 for the model given by Eqs. (24) and $k_B T = \Gamma/100$. The curves for different values of the parameter ξ are obtained with the Eqs. (A4)–(A7). Note that $\xi_{\uparrow\downarrow} = \{1,0\}$ for $\xi = 1$ and $\xi_{\uparrow\downarrow} = \{1/2,1/2\}$ for $\xi = 0$, respectively.

$$S(t) = \frac{\Gamma_L(t)}{2}[f(t)[2 - 3n_s(t) - 2r(t) - \xi\,\delta n(t) \times [1 - 2r(t)/n_s(t)]] + [n_s(t) - 2r(t)] \times [1 + \xi\,\delta n(t)/n_s(t)]], \tag{A5}$$

where we have used an auxiliary quantity $r(t) \equiv p'_\uparrow(t) + p'_\downarrow(t) - n(t)[p'_0(t) + p'_\uparrow(t) + p'_\downarrow(t)]$, which is the generalized version of Eqs. (8). The corresponding equations of motion for the occupation and the polarization read

$$\frac{\partial}{\partial t} n_s(t) = \frac{\Gamma(t)}{2}[f(t)[2 - n_s(t) + \xi\,\delta n(t)] - [n_s(t) + \xi\,\delta n(t)]], \tag{A6a}$$

$$\frac{\partial}{\partial t} \delta n(t) = \frac{\Gamma(t)}{2}[f(t)[\delta n(t) + \xi[2 - n_s(t)]] - [\delta n(t) + \xi\, n_s(t)]]. \tag{A6b}$$

To close the set of equations of motion we need an equation for $r(t)$, which reads

$$\frac{\partial}{\partial t} r(t) = \frac{\Gamma_L(t)}{2}(f(t)\{2 - n_s(t)[4 - n_s(t) + \xi\,\delta n(t)] + n_s(t)[n_s(t) + \xi\,\delta n(t)]\}) - \frac{\Gamma(t)}{2} r(t)\{[f(t) + 1] + \xi\,\bar{f}(t)\delta n(t)/n_s(t)\}. \tag{A7}$$

This is the generalized set of equations describing the time-dependent current and noise and the respective quantities like level occupations and polarization.

It can easily be checked that for $\xi = \pm 1$ the above set of equations reduces to those give in Sec. II A, with n_s replaced by $n_{\uparrow\downarrow}$ and δn replaced by $\pm n_{\uparrow\downarrow}$, respectively.

For the unpolarized case $\xi = 0$, one gets

$$I(t) = \frac{\Gamma_L(t)}{2}\{f(t)[2 - n_s(t)] - n_s(t)\}, \tag{A8}$$

$$S(t) = \frac{\Gamma_L(t)}{2}\{2[f(t) - n_s(t)] + 3\bar{f}(t)n_s(t) - 2[1 + f(t)]r(t)\}, \tag{A9}$$

with

$$\frac{\partial}{\partial t} n_s(t) = -\frac{\Gamma(t)}{2}\{n_s(t) - f[2 - n_s(t)]\}, \tag{A10a}$$

$$\frac{\partial}{\partial t} r(t) = \frac{\Gamma_L(t)}{2}\left(n_s{}^2(t) + f(t)\{2 - n_s(t)[4 - n_s(t)]\}\right) - \frac{\Gamma(t)}{2} r(t)[1 + f(t)]. \tag{A10b}$$

Note that $\delta n(t) \to 0$ in this case.

The instantaneous solutions, i.e., assuming that all time derivatives vanish, read

$$n_s(t) = \frac{2f(t)}{1 + f(t)}, \tag{A11a}$$

$$\delta n(t) = 0, \tag{A11b}$$

$$r(t) = \frac{\Gamma_L(t)}{\Gamma(t)} \frac{2f(t)\bar{f}(t)}{[1 + f(t)]^2}, \tag{A11c}$$

which turn out to be independent of ξ. It follows for the noise that

$$S(t) = \frac{\Gamma_L(t)\Gamma_R(t)}{\Gamma(t)} \frac{2f(t)\bar{f}(t)}{1 + f(t)}. \tag{A12}$$

Comparing the expressions for n_s and S with the ones given in Sec. II C, one sees that the main difference is the factor $1 + f$ in the denominator. The noise per period can be obtained analogous to Eq. (23). In particular the proportionality to $k_B T/\Omega$ remains valid.

In Fig. 5 a comparison of the results described in Sec. III for exponential modulation ($\xi = 1$) and results for the unpolarized

case ($\xi = 0$) are shown. One finds that the results are qualitatively very similar. For $\delta \neq 0$ the curves $Q(\Omega)$ and $\Delta Q^2(\Omega)$ in the unpolarized case are shifted toward smaller frequencies compared to the polarized case.

[1] J. Flowers, Science **306**, 1324 (2004).
[2] M. W. Keller, Metrologia **45**, 102 (2008).
[3] M. D. Blumenthal, B. Kaestner, L. Li, S. Giblin, T. J. B. M. Janssen, M. Pepper, D. Anderson, G. Jones, and D. A. Ritchie, Nat. Phys. **3**, 343 (2007).
[4] A. Fujiwara, K. Nishiguchi, and Y. Ono, Appl. Phys. Lett. **92**, 042102 (2008).
[5] B. Kaestner, V. Kashcheyevs, S. Amakawa, M. D. Blumenthal, L. Li, T. J. B. M. Janssen, G. Hein, K. Pierz, T. Weimann, U. Siegner, and H. W. Schumacher, Phys. Rev. B **77**, 153301 (2008).
[6] S. P. Giblin, S. J. Wright, J. D. Fletcher, M. Kataoka, M. Pepper, T. J. B. M. Janssen, D. A. Ritchie, C. A. Nicoll, D. Anderson, and G. A. C. Jones, New J. Phys. **12**, 073013 (2010).
[7] S. Giblin, M. Kataoka, J. Fletcher, P. See, T. Janssen, J. Griffiths, G. Jones, I. Farrer, and D. Ritchie, Nat. Commun. **3**, 930 (2012).
[8] L. Fricke, M. Wulf, B. Kaestner, F. Hohls, P. Mirovsky, B. Mackrodt, R. Dolata, T. Weimann, K. Pierz, U. Siegner, and H. W. Schumacher, Phys. Rev. Lett. **112**, 226803 (2014).
[9] N. Ubbelohde, F. Hohls, V. Kashcheyevs, T. Wagner, L. Fricke, B. Kästner, K. Pierz, H. W. Schumacher, and R. J. Haug, Nat. Nanotechnol. **10**, 46 (2015).
[10] B. Kaestner and V. Kashcheyevs, Rep. Prog. Phys. **78**, 103901 (2015).
[11] C. Emary and R. Aguado, Phys. Rev. B **84**, 085425 (2011).
[12] D. A. Bagrets and Y. V. Nazarov, Phys. Rev. B **67**, 085316 (2003).
[13] A. Braggio, J. König, and R. Fazio, Phys. Rev. Lett. **96**, 026805 (2006).
[14] T. Novotný, J. Comput. Electron. **12**, 375 (2013).
[15] D. A. Ivanov, H. W. Lee, and L. S. Levitov, Phys. Rev. B **56**, 6839 (1997).
[16] A. G. Abanov and D. A. Ivanov, Phys. Rev. Lett. **100**, 086602 (2008).
[17] M. Esposito, U. Harbola, and S. Mukamel, Rev. Mod. Phys. **81**, 1665 (2009).
[18] F. Pistolesi, Phys. Rev. B **69**, 245409 (2004).
[19] C. Flindt, T. Novotný, and A.-P. Jauho, Europhys. Lett. **69**, 475 (2005).
[20] S. D. Bennett and A. A. Clerk, Phys. Rev. B **78**, 165328 (2008).
[21] G. B. Lesovik and L. S. Levitov, Phys. Rev. Lett. **72**, 538 (1994).
[22] S. Camalet, J. Lehmann, S. Kohler, and P. Hänggi, Phys. Rev. Lett. **90**, 210602 (2003).
[23] B. H. Wu and C. Timm, Phys. Rev. B **81**, 075309 (2010).
[24] N. Maire, F. Hohls, B. Kaestner, K. Pierz, H. W. Schumacher, and R. J. Haug, Appl. Phys. Lett. **92**, 082112 (2008).
[25] P. W. Brouwer, Phys. Rev. B **58**, R10135(R) (1998).
[26] F. Zhou, B. Spivak, and B. Altshuler, Phys. Rev. Lett. **82**, 608 (1999).
[27] O. Entin-Wohlman, A. Aharony, and Y. Levinson, Phys. Rev. B **65**, 195411 (2002).
[28] M. Moskalets and M. Büttiker, Phys. Rev. B **64**, 201305 (2001).
[29] F. Cavaliere, M. Governale, and J. König, Phys. Rev. Lett. **103**, 136801 (2009).
[30] R.-P. Riwar, J. Splettstoesser, and J. König, Phys. Rev. B **87**, 195407 (2013).
[31] T. Yuge, T. Sagawa, A. Sugita, and H. Hayakawa, Phys. Rev. B **86**, 235308 (2012).
[32] R. Yoshii and H. Hayakawa, arXiv:1312.3772.
[33] A. Croy, U. Saalmann, A. R. Hernández, and C. H. Lewenkopf, Phys. Rev. B **85**, 035309 (2012).
[34] A. Croy and U. Saalmann, Phys. Rev. B **86**, 035330 (2012).
[35] S. A. Gurvitz and Y. S. Prager, Phys. Rev. B **53**, 15932 (1996).
[36] A. V. Andreev and E. G. Mishchenko, Phys. Rev. B **64**, 233316 (2001).
[37] Y. M. Blanter and M. Büttiker, Phys. Rep. **336**, 1 (2000).
[38] M. Büttiker, Phys. Rev. Lett. **65**, 2901 (1990).